# Flame Synthesis of Carbon Nanotubes Using a Double-faced Wall Stagnation Flow Burner

S.K. Woo[*], Y.T. Hong[**], and O.C. Kwon[***]

[*]Sungkyunkwan University, Suwon, Kyunggi-do, Korea, wooday2@naver.com
[**]Sungkyunkwan University, Suwon, Kyunggi-do, Korea, hongyt1999@naver.com
[***]Sungkyunkwan University, Suwon, Kyunggi-do, Korea, okwon@skku.edu

## ABSTRACT

The potential of using a double-faced wall stagnation flow burner in mass production of carbon nanotubes was evaluated experimentally and computationally. With nitrogen-diluted premixed ethylene-air flames established on the Nickel-coated stainless steel double-faced wall, the propensities of carbon nanotube formation were experimentally determined using SEM and FE-TEM images and Raman spectroscopy, while the flame structure was computationally predicted using a 3-dimensional CFD code with a reduced reaction mechanism. The uniformity and yields of synthesized carbon nanotubes were evaluated in terms of the flame stretch rates. Results show substantial increase of area on the wall surface where uniform carbon nanotubes are synthesized with using the double-faced wall stagnation flow burner due to enhanced uniformity of temperature distribution along the wall surface and support the potential of using a double-faced wall stagnation flow burner in mass production of carbon nanotubes.

***Keywords***: combustion synthesis, CNTs, double-faced wall stagnation flow burner

## 1 INTRODUCTION

Because of the unique mechanical and electrical properties of carbon nanotubes (CNTs), there has been substantial interest in their use for a wide variety of new applications, including field emission displays, gas sensors and hydrogen storage materials for fuel cells [1, 2]. Consequently extensive fundamental research has been conducted on the synthesis of CNTs since the discovery of these nanostructures in 1991 [1, 3]. Recently, in response to the concern at mass production of CNTs, there is also increasing interest in the synthesis of them using combustion [4-14].

Vander Wal and coworkers investigated effects of various catalysts, catalyst particle structure and reactant gas mixtures on the growth and structure of single-walled CNTs and carbon nanostructures for nonpremixed flames [4]. They also synthesized single-walled and multi-walled CNTs for premixed coflow flames [5, 6]. Saito and coworkers employed coflow and counterflow nonpremixed flames for the growth of multi-walled CNTs on catalytic supports inserted into flames [7, 8]. Synthesis of CNTs was observed in oxygen-enriched counterflow nonpremixed flames without a catalyst by Kennedy and coworkers [9]. They also demonstrated that well aligned CNTs can be synthesized in electric field [10]. Height et al. determined the conditions at which single-walled CNTs are synthesized in terms of flame position and fuel-equivalence ratios in a premixed one-dimensional flame [11]. Lee et al. [12] and Xu et al. [13] synthesized multi-walled CNTs in inverse nonpremixed flames. Even the synthesis of CNTs in ethanol flames using the common combustion apparatus with a wick was reported [14].

The earlier investigations have been focused on the fundamental aspects of combustion synthesis of CNTs for various flame configurations. Considering that the combustion synthesis methods have potential for mass production of CNTs, however, a unique method that can be directly applicable to mass production of CNTs should be developed. Recently, such an attempt for mass production was reported by Nakazawa et al. [15]. Instead of using small catalytic supports to collect CNTs, a stagnation wall was used for CNTs synthesis. It was observed that abundant multi-walled CNTs were synthesized on a doughnut-shaped area of the wall surface.

We propose herein an alternate flame configuration towards enabling mass production of CNTs. A double-faced wall stagnation flow (DWSF) burner establishes a premixed flame above each side of a stagnation wall since the diluted fuel-air premixtures injected through upper and lower nozzles are ignited, respectively (see Fig. 1). The combustion of these mixtures appears to possess some potentially beneficial characteristics.

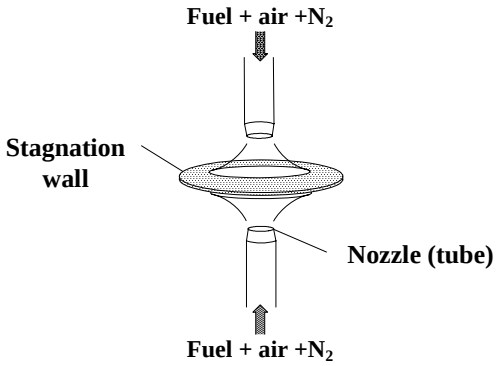


Figure 1: Sketch of a double-faced wall stagnation flow (DWSF) burner.



NSTI-Nanotech 2007, www.nsti.org, ISBN 1420061828 Vol. 1, 2007

First, similar to the single-faced wall stagnation flow (SWSF) burner suggested by Nakazawa et al. [15], the DWSF burner may produce abundant CNTs. Second, since two flames are generated along both surfaces of the stagnation wall, heat losses through the wall can be minimized, saving a cost of CNT mass production. Furthermore, the unique configuration of the DWSF burner-generating flames can redistribute temperature profiles on the wall surfaces by properly controlling stretch rates of flames through changing mass flow rates of premixtures at the upper and lower nozzles or the distance between the nozzle and the wall. The temperature profiles on the stagnation wall surface are considered one of critical parameters influencing the quality of synthesized CNTs.

In view of the above considerations, in the present investigation we aim to study the potential of improving mass production of CNTs by using a DWSF burner, with the following specific objectives. The first is to measure the propensities of SWSF burner-generating CNT formation such as yields and internal structure, as a baseline condition. The second is to predict the structure of the SWSF burner-generating flame by using a 3-dimensional CFD code with a reduced reaction mechanism. The third is to experimentally and computationally observe the effects of using the DWSF burner instead of the SWSF burner on the properties of synthesized CNTs. We shall also examine the effects of stretch rates of flames on the formation of CNTs. The study was conducted for a wide range of stretch rates and a fixed fuel-equivalence ratio.

## 2 EXPERIMENTAL AND COMPUTATIONAL METHODS

The premixed flames established on a DWSF burner were adopted for the present investigation on synthesis of CNTs due to the aforementioned potential benefits such as mass production of CNTs, minimized heat losses and easy quality control of synthesized CNTs. A diagram of the present experimental apparatus appears in Fig. 2, which consists of upper and lower tubes surrounded by water-cooling pipes, a stagnation wall (plate), a reactant mixture supply system and a digital camera (Nikon D70) for recording the flame images.

Premixture jets issued from stainless steel (SS304) tubes with inner diameter (d) of 6 mm and with the passage length/diameter ratio of 100 to help insure fully-developed laminar pipe flow at the tube exit are impinged on a flat stagnation wall and then spark-ignited so that premixed flames are formed above both the wall surfaces. Mass flow meters (Dwyer: 0.5 and 5.0 slm) with accuracy ±4% of full scale delivered the combustible mixture to the tubes, independently controlling mixture composition (fuel-equivalence ratio $\phi$) and tube exit velocity V. Varying the jet velocities at the tube exit and/or the distance between the stagnation plate and the tube exit, flame stretch rates could be controlled within a range of stabilizing stationary flames. The global stretch rate is defined as follows:

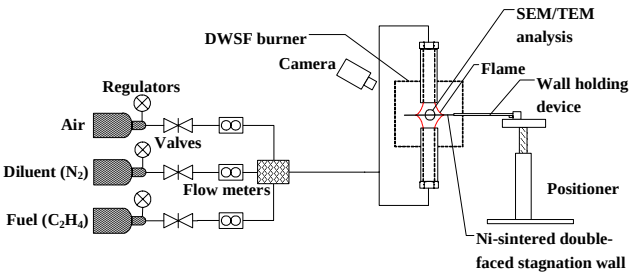


Figure 2: Schematic of experimental apparatus for the CNT synthesis.

$$\kappa = V/s \qquad \left[s^{-1}\right] \tag{1}$$

where s is the distance between the stagnation plate and the tube exit. A Nickel (Ni)-coated stainless steel disk with diameter of 45 mm and thickness of 0.7 mm was used. The plate was coated by Ni powder with diameter of 3 μm using the pulse electric current sintering process. The Ni-coated plate surface heated by the flames was exposed to the premixture: the exposure time varied from 3 to 10 min since time to accumulate a certain quantity of the CNTs on the surface is up to the test condition.

Synthesized CNTs were analyzed using SEM (Philips ESEM-FEG-XL30), FE-TEM (Joel JEM2100F) and Raman spectroscopy (RS, Kaiser Optical). For the TEM analysis, the deposited CNTs were scraped off the plate surface and adhered onto TEM grids and then the images were taken, while for the SEM and RS analyses, the images were directly taken.

Nitrogen ($N_2$)-diluted ethylene ($C_2H_4$)/air premixed flames were established at temperature T = 298±3 K and atmospheric pressure (NTP): the diluent was used to control the flame temperature. The tubes (and thus reactants) were maintained at room temperature by water-cooling. Experiments were carried for $\phi$ = 1.6 and V = 1.2-2.6 m/s, resulting in $\kappa$ = 147-648 $s^{-1}$. For all the test conditions, the reproductivity was confirmed by measurements of 3 to 4 tests at each condition.

The premixed flames stabilized on a DWSF burner were simulated using a commercially available CFD code FLUENT 6.2 [16]. The time-dependent ordinary sets of the continuity equation, the cylindrical two-dimensional (cylindrical: r-x, where r and x are the radial and axial coordinates, respectively) Navier-Stokes equations, the energy conservation equation and the species conservation equations were solved with the finite volume method. The code allows for multi-component diffusion, thermal diffusion, variable thermochemical properties and variable transport properties. The CHEMKIN database was used to find the thermochemical properties [17]. $N_2$-diluted $C_2H_4$ and air ($21\%O_2/79\%N_2$ in volume) mixtures were considered with a reduced 10-step reversible $C_2H_4/O_2$ reaction mechanism involving 10 species due to Singh and

Jachimowski (1994) [18]. Surface reactions on the catalytic plate were not considered for the present study, since any reliable reaction mechanism of $C_2H_4/O_2$ on the Ni surface is not available in the literature and the numerical simulations were conducted only for the purpose of determining experimental test conditions and comparing the gas phase flame structure including plate surface temperature for the DWSF burner with one for the SWSF burner.

The governing equations adapting the above submodels were discretized and simultaneously solved [16]. The current entire region of calculations is 27d and 40d for the radial and axial directions, respectively (total number of 70,000 grid points). Parabolic flow of a diluted fuel-air mixture is injected into a still air at NTP. The parallel computation system consisted of 16 personal computers (CPU speed of 3.0 GHz each) allowed for the two dimensional computations with the submodels.

## 3 RESULTS AND DISCUSSION

Figure 3 shows the SEM and FE-TEM images of the carbon materials formed on the Ni-coated plate surface at r = 18 mm for a premixed $C_2H_4/O_2/N_2$ flame of $\phi$ = 1.6, V = 1.2 m/s, s = 6.0 mm (resulting in $\kappa$ = 196 $s^{-1}$) and the volumetric $O_2$ concentration in the nonfuel gases $X_{O2}$ = 0.123 that was generated from an upwardly issued SWSF burner. The exposure time to obtain the CNTs was 10 min. The images indicate that the synthesized carbon materials are hollow-centered multi-walled CNTs (MWNTs) with the diameters in the range of several to tens nanometers. The MWNTs were observed in a doughnut-shaped region of r = 12-20 mm. Considering that there are temperature and supplied gas mixture conditions suitable for the CNT synthesis, it is interesting to observe that the doughnut-shaped region is roughly identical to the region where the predicted temperature distribution along plate surface is nearly uniform as shown in Fig. 4 (though computations were conducted for $X_{O2}$ = 0.184 that is higher than experimental condition, due to computational instability).

Figure 5 shows the SEM and FE-TEM images and the Raman spectrum of the CNTs formed on the Ni-coated plate surface at r = 18 mm for a premixed $C_2H_4/O_2/N_2$ flame of $\phi$ = 1.6, the upper tube exit velocity $V_u$ = 2.6 m/s, the lower tube exit velocity $V_l$ = 1.2 m/s, s = 6.0 mm

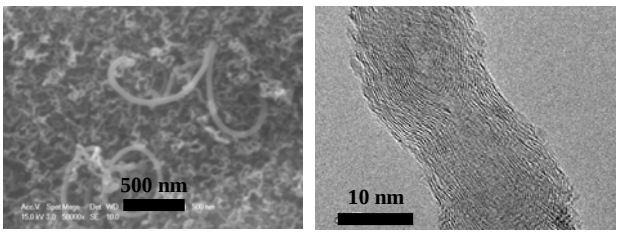


Figure 3: SEM and FE-TEM images of the CNTs formed on the Ni-coated plate surface: r = 18 mm, $\phi$ = 1.6, V = 1.2 m/s, s = 6.0 mm ($\kappa$ = 196 $s^{-1}$) and $X_{O2}$ = 0.123 (an upwardly issued mixture).

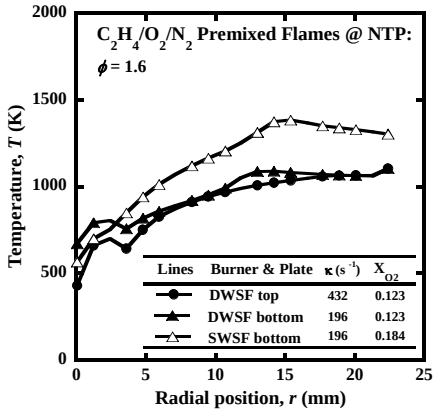


Figure 4: Predicted temperature distribution along the stagnation plate surface for the flames used in Fig. 5.

(resulting in $\kappa_u$ = 432 $s^{-1}$ and $\kappa_l$ = 196 $s^{-1}$ for the downwardly and upwardly issued mixtures, respectively) and $X_{O2}$ = 0.123 that was generated from a DWSF burner. The different stretch rates for the upper and lower flames were determined from balancing the CNTs-generated regions on the upper and lower surfaces for various conditions. The TEM image indicates that the synthesized carbon materials are MWNTs with the averaged diameter of 17 nm. However, the Raman spectrum shows the synthesized MWNTs (G-band) with some defective graphite layers at walls (D-band). Considering various TEM images (not shown here), the present MWNTs seem to grow according to a base growth model due to a weak affinity of Ni to carbon [14]. Figures 5 (a-c) and (d) are for the CNTs synthesized on the top and bottom surfaces, respectively. For each surface, MWNTs of relatively uniform and similar quality were observed in a broadened

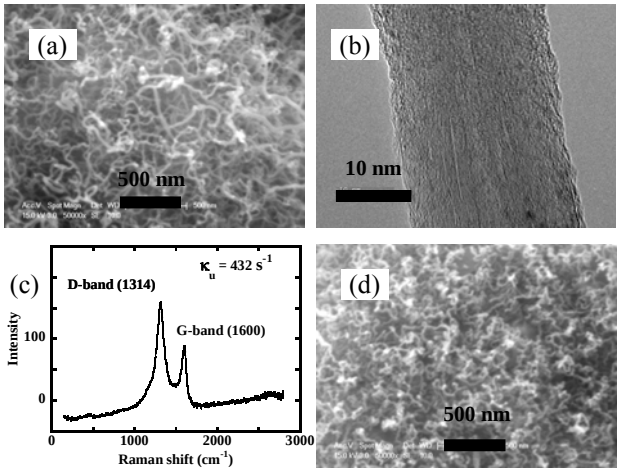


Figure 5: SEM and FE-TEM images and Raman spectrum of the CNTs formed on the top (a-c) and bottom (d) surfaces: r = 18 mm, $\phi$ = 1.6, $V_u$ = 2.6 m/s, $V_l$ = 1.2 m/s, s = 6.0 mm ($\kappa_u$ = 432 $s^{-1}$ and $\kappa_l$ = 196 $s^{-1}$) and $X_{O2}$ = 0.123.


NSTI-Nanotech 2007, www.nsti.org, ISBN 1420061828 Vol. 1, 2007

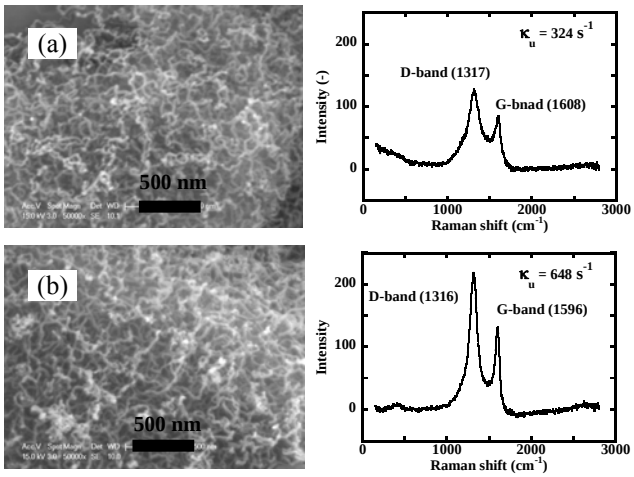


Figure 6: Effects of flame stretch rates on the formation of CNTs (for the same mixture as in Fig. 5): (a) $\kappa_u$ = 324 $s^{-1}$, $\kappa_l$ = 147 $s^{-1}$ and s = 8.0 mm; (b) $\kappa_u$ = 648 $s^{-1}$, $\kappa_l$ = 295 $s^{-1}$ and s = 4.0 mm. The results for the top surface are shown.

range (r = 14-22.5 and 11-18 mm for the top and bottom surfaces, respectively), compared to the corresponding CNTs generated for a SWSF burner shown in Fig. 3. This observation is also confirmed from the broadened uniform temperature range shown in Fig. 4. The exposure time to obtain the CNTs was 5 min, which is much shortened than that for the corresponding SWSF burner. Thus, the unique configuration of the DWSF burner-generating flames redistributes temperature profiles on the wall surfaces, improving the quality and yields of CNTs compared to the corresponding SWSF burner-generating flame. In addition, since two flames are generated along both surfaces of the stagnation wall, heat losses across the wall were minimized, enhancing the yields of CNTs. The temperature profiles on the stagnation wall surface are considered one of critical parameters influencing the quality of synthesized CNTs.

In order to examine the effects of stretch rates of flame on the formation of CNTs, the experiments were conducted for the same mixture as one in Fig. 5. The results for the top surface are shown in Fig. 6: (a) $\kappa_u$ = 324 $s^{-1}$, $\kappa_l$ = 147 $s^{-1}$ and s = 8.0 mm (the exposure time = 7 min), and (b) $\kappa_u$ = 648 $s^{-1}$, $\kappa_l$ = 295 $s^{-1}$ and s = 4.0 mm (the exposure time = 3 min). Comparing these results to the baseline one in Fig. 5, the optimized stretch rate for preferred quality of CNTs may exist. For example, if straight CNTs are preferred, the present limited data show that the best quality of CNTs is observed for $\kappa_u$ = 432 $s^{-1}$ and $\kappa_l$ = 196 $s^{-1}$. Considering that the region where CNTs are uniformly synthesized is broadened and the exposure time for synthesis is shortened with increasing stretch rates, however, higher stretch rates are better for yields of CNTs unless the outer region of synthesis becomes out of the plate size. Meanwhile, less stretched flames synthesize CNTs with less defective graphite layers at walls. Thus, depending on the preferred quality of CNTs, we can determine the stretch rate of flame.

# 4 CONCLUDING REMARKS

We proposed an alternate flame configuration towards enabling mass production of CNTs, DWSF burner-generating flame. Substantial increase of area on the wall surface where uniform carbon nanotubes are synthesized with using the DWSF burner due to enhanced uniformity of temperature distribution along the wall surface was observed, supporting the potential of using a DWSF burner in mass production of CNTs. Since the present study showed that enhanced stretch rates improve yields of CNTs with more defective graphite layers at walls, the optimized stretch rate should be determined depending on preferred quality of synthesized CNTs.

*This work was supported by the Korean Research Foundation Grant (KRF-2006-311-D00341) funded by the Korean Government (MOEHRD).*

[1] F.E. Kruis, H. Fissan and A. Peled, J. Aerosol Sci. 29, 511-535, 1998.
[2] C.-H. Chen and C.-C. Huang, Int. J. Hydrogen Energy 32, 237-246, 2007.
[3] S. Iijima, Nature 354, 56-58, 1991.
[4] R.L. Vander Wal and J.H. Lee, Chem. Phys. Lett. 349, 178-184, 2001.
[5] R.L. Vander Wal, Combust. Flame 130, 37-47, 2002.
[6] R.L. Vander Wal, J.H. Lee and G.M. Berger, Proc. Combust. Inst. 29, 1079-1085, 2002.
[7] L. Yuan, K. Saito, C. Pan, F.A. Williams and A.S. Gordon, Chem. Phys. Lett. 340, 237-241, 2001.
[8] T.X. Li, H.G. Zhang, F.J. Wang, Z. Chen and K. Saito, Proc. Combust. Inst. 31, 1849-1856, 2007.
[9] W. Merchan-Merchan, A. Saveliev, L.A. Kennedy and A. Fridman, Chem. Phys. Lett. 354, 20-24, 2002.
[10] W. Merchan-Merchan, A. Saveliev and L.A. Kennedy, Carbon 44, 3308-3314, 2006.
[11] M.J. Height, J.B. Howard, J.W. Tester and J.B. Vander Sande, Carbon 42, 2295-2307, 2004.
[12] G.W. Lee, J. Jurng and J. Hwang, Combust. Flame 139, 167-175, 2004.
[13] F. Xu, X. Liu and S.D. Tse, Carbon 44, 570-577, 2006.
[14] C. Pan, Y. Liu, F. Cao, J. Wang and Y. Ren, Micron 35, 461-468, 2004.
[15] S. Nakazawa, T. Yokomori and M. Mizomoto, Chem. Phys. Lett. 403, 158-162, 2005.
[16] Fluent Inc., "Fluent 6.2 User's Guide," Fluent Inc., U.S.A., 2001.
[17] R.J. Kee, F.M. Rupley and J.A. Miller, "The CHEMKIN Thermodynamic Data Base," Report No. SAND87-8215B, Sandia National Laboratories, 1992.
[18] D.J. Singh and C.J. Jachimowski, AIAA J. 32, 213-216, 1994.